Nuclear Instruments and Methods in Physics Research A243 (1986) 459–464
North-Holland, Amsterdam

STUDY OF A PROTOTYPE XENON TPC

M.A. IQBAL, B. O'CALLAGHAN, H. HENRIKSON and F. BOEHM

Norman Bridge Laboratory of Physics 161-33, California Institute of Technology, Pasadena, California 91125, USA

Received 7 August 1985

The design, construction and performance of a 16-channel xenon time projection chamber (TPC) of about 1 l volume is discussed. This prototype TPC was able to provide sufficient information regarding scintillation, energy resolution and track reconstruction for the development of the next generation TPC, suitable for double beta decay experiments.

1. Introduction

Neutrinoless double beta decay has long been recognized as a very sensitive tool to search for the nonconservation of lepton number. Recently, the interest in this process has been renewed by the possibility of a finite neutrino mass and right-handed currents in weak decays.

Double beta decay can occur via the two-neutrino mode, $(A, Z) \rightarrow (A, Z+2) + 2e + 2\bar{\nu}$ as well as the zero-neutrino mode, $(A, Z) \rightarrow (A, Z+2) + 2e$. The two-neutrino double beta decay mode is a standard second order beta decay, whereas the zero-neutrino mode involves nonconservation of lepton number. This neutrinoless channel is capable to explore the Majorana neutrino mass range down to 1 eV or less, and right-handed currents admixture to below 10^{-5} in amplitude.

There are two classes of double beta decay experiments that have been carried out since 1949 [1–5]. The first class involves geochemical analysis of minerals with a geological age of about 10^9 years, searching for abnormal abundance of the isotope $(A, Z+2)$ in the isotope (A, Z). These experiments have given positive evidence for double beta decay in the isotopes ^{82}Si [6], ^{130}Te [7,8] and perhaps in ^{128}Te [9,10]. However, geochemical experiments are unable to distinguish the two-neutrino mode from the zero-neutrino mode. Moreover, it has been argued that processes other than double beta decay cannot always be ruled out as being responsible for the abnormal abundance of the isotope $(A, Z+2)$.

The second class of experiments involves the detection of the two electrons from double beta decay. The neutrinoless mode can be distinguished from the two-neutrino mode by the total energy of the electrons. All of the energy in the neutrinoless mode goes to the two electrons while in the two-neutrino mode all four leptons share the total energy. To date there is no laboratory evidence for neutrinoless double beta decay. Two-neutrino double beta decay, on the other hand, may have been seen recently in a laboratory experiment in ^{82}Se [11]. At present the best laboratory lifetimes limits in double beta decay have been obtained in ^{76}Ge [12]. Groups at Caltech [13], Milan [14], Battelle [15], Santa Barbara [16], Osaka [17] and Guelph [18] are currently conducting experiments with germanium to search for the elusive neutrinoless decay. Once the background counts have been sufficiently reduced, the ultimate limitation in these experiments is the number of ^{76}Ge atoms in the detector. In order to make further progress larger systems with more atoms have to be considered.

The number of available isotopes in nature for double beta decay is rather limited and among them ^{136}Xe seems to be a very promising case for the following reasons:

(1) The natural abundance of ^{136}Xe is 8.87%, and it is possible to have a system with a very large number of atoms without isotopic enrichment. (^{136}Xe can also be obtained as an enriched isotope since it is produced as a fission product at nuclear power plants).

(2) The Q value for ^{136}Xe (2.48 MeV) is slightly higher than that of ^{76}Ge (2.04 MeV) which increases the rate due to the phase space factor.

(3) Since xenon is a noble gas it can be used in a TPC and similar to a germanium detector, the detector will be the source. The TPC can be operated with liquid or solid xenon where the very high energy resolution will discriminate against the background. In a high pressure gas TPC, an excellent background rejection can be achieved by the track recognition capabilities along with the energy loss $(\mathrm{d}E/\mathrm{d}x)$ considerations. A double beta decay event will be identified by the two electron tracks with a common vertex. Although multiple scattering complicates the recognition of such a vertex, the ends of the tracks can be recognized by the charge blobs due to the increased $\mathrm{d}E/\mathrm{d}x$ for low energy electrons.

In this report we describe the results of a small

prototype xenon TPC of about 1 l volume with 16 channels, operated at 1 atm pressure. We are in the process of designing a 400 channel high pressure gas TPC for the double beta decay experiment.

2. Construction

2.1. Prototype TPC

The prototype TPC is shown in fig. 1. It consists of a 10 cm cathode plane made of copper and separated by two field shaping rings and a Frisch grid. The field shaping rings are connected to a voltage divider to obtain a uniform electric field inside the TPC. The Frisch grid is kept at ground potential to isolate the readout system from the drift region. This drift region is mounted on a Delrin slab which holds the 16-channel readout system. The readout system consists of 8 anode wires (diameter 0.002 cm), 1 cm apart, with guard wires (diameter 0.005 cm) in between to reduce the crosstalk between the anode wires. The pads, perpendicular to the anode wires, are made of eight 1 cm copper strips and mounted on the Delrin slab with high vacuum epoxy. The readout system along with the drift region is mounted on a conflat flange and the whole assembly is placed inside a stainless steel vessel of about 1 l volume. An ultraviolet photomultiplier tube looks into the system through a sapphire window in order to study the scintillation light.

2.2. The gas handling system

The gas handling system for the prototype TPC consists of a gas purifier, a circulating pump, a high vacuum pumping stage, a gas manifold, and reservoirs for gas storage as shown in fig. 2. The system is designed to pump down to high vacuum before introducing the fill gas. An on-line mass spectrum analyzer (Model M-100, Dycor Electronics Inc.) is connected to the system to monitor possible contaminants. Since xenon is very susceptible to contamination the gas must be

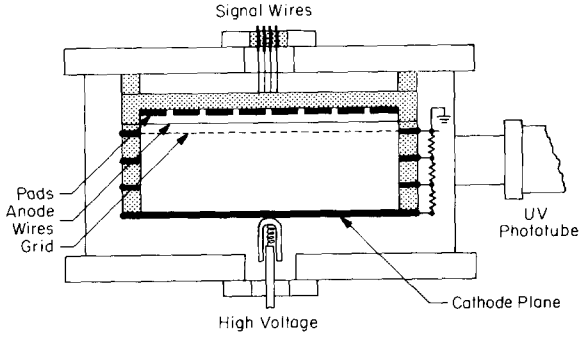

Fig. 1. Schematic diagram of the prototype xenon TPC.

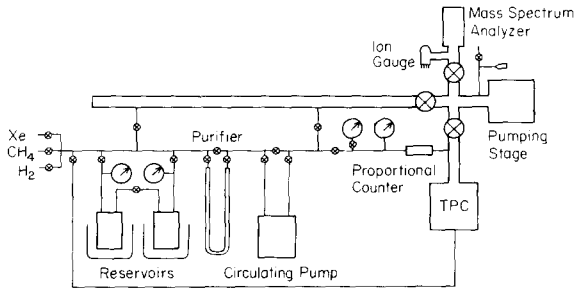

Fig. 2. The gas handling system.

circulated through a purifier for constant purification. We use a metal bellows pump (Model MB-302, Metal Bellows Corp.) for the recirculation. Initially a commercial purifier (Hydrox Purifier, Model 8301) was used to remove contaminants like O_2 and water vapours. However, this purifier removes N_2 from the gas mixture and since we wanted to make measurements with N_2 as an admixture, we built our own purification system.

Our system can be operated at room temperature and it can be regenerated very simply once it gets overloaded. The purifier consists of two stainless steel columns containing MnO and molecular sieve (4A). The MnO removes O_2 from the circulating gas while the molecular sieve traps water molecules. Both O_2 and water molecules are particularly unwanted since they are electronegative and can remove drifting electrons by the formation of negative ions. The gas handling system also has two stainless steel reservoirs where the fill gas can be condensed with liquid nitrogen. The two reservoirs were found to be very useful for temporary storage and purification of certain gas mixtures by fractional distillation during various studies.

2.3. The readout electronics

The anode wires produce a negative pulse during charge multiplication, a current sensitive preamplifier (based on LeCroy TRA 1000) is used to obtain a fast pulse of a few hundred ns time constant. The pulses from the pads have opposite polarity since they are produced by the image charges. We have used the inverted output from the preamplifier for the pads so that the signals from all the channels have the same polarity. The preamplifier signals are then shaped and amplified by shaping amplifiers. In the final design of the TPC we will require an independent waveform digitizer at this stage for each channel. Since at the present time we have not constructed these, we can not have precise information about the total energy or dE/dx. However, using the available electronics we were able to reconstruct tracks of charged particles. To do this, the output signals of the shaping amplifiers are

converted into TTL signals. At this point we lose all the energy information from the pulses and they are used for timing purposes only. The TTL signals from the anode wires and the pads are then fed into two 2K × 8 RAM ICs so that each bit of the 8-bit word corresponds to a channel. A start (or time zero) signal enables the RAM ICs to write into them and at the same time the address starts incrementing with a 5 MHz clock so that each address corresponds to a time bucket of 200 ns. The address counter stops after a predetermined time and the status of each channel is stored in the RAM as a function of time. The RAMs are read by the computer (PDP 11/23) using a CAMAC dataway. We have designed a simple CAMAC decoder which interfaces the RAMs and the associated electronics with the computer.

3. Results

3.1. Scintillation

Xenon is a very good scintillator, the light output from xenon is about seven times larger than that of argon [19]. The process of scintillation is rather complex and involves the formation of diatomic molecules [20–22] due to three-body collisions. The spectrum is quite broad (1475–2200 Å) and the sharp atomic lines at 1473 Å can be seen only at very low pressure. Originally we had planed to use the primary scintillation as time zero trigger in the TPC. For this reason we studied the scintillation in great detail. However, it turned out that good imaging and energy resolution is in conflict with the requirement of good scintillation yield, as described below.

The xenon scintillates in the far UV region and the detection is somewhat complicated. One requires either a phototube with a special UV window (e.g. MgF_2, LiF_2) or a wavelength shifter in conjunction with ordinary glass window photomultiplier tube. We tried different wavelength shifters, e.g. p-Quaterphenyl, p-Terphenyl and Tetraphenyl butadiene, and found that all of these work very well, especially scintillation grade Tetraphenyl butadiene. We coated a pyrex glass window with the wavelength shifters by vapour deposition and found the UV-to-visible conversion to be quite insensitive to film thickness in a range from 50 to 300 $\mu g/cm^2$. However, these wavelength shifters are organic compounds and may have noticeable vapour pressures. To use them inside a system containing very pure xenon requires special precautions, such as coating the wavelength shifter with a thin layer of MgF_2.

Pure xenon has the maximum light output, but inside a TPC one can not use it in pure form since the drift velocity of electrons in pure xenon is known to be small [23] and consequently the diffusion of the electrons is large. This experiment under consideration is not a high count rate experiment, so large drift velocities to sweep charges as soon as possible are not essential. However, the diffusion of electrons in pure xenon is a serious limitation even with our modest requirement of 3 mm spatial resolution. Electrons diffuse almost 1 cm [24] in 1 m drift distance in pure xenon at atmospheric pressure with an electric field of 100 V/cm. The diffusion rate can be reduced by adding hydrocarbons (CH_4) or molecular gases (CO_2) which thermalize the electrons.

We studied the scintillation of xenon (and argon for comparison) with different gas mixtures which might be suitable for improving the drift and diffusion properties. The results are shown in fig. 3 for N_2, H_2 and CO_2 admixtures with xenon and argon. The results of mixing CH_4 and C_2H_4 are not shown in the figures since very little admixtures (less than 1%) of these hydrocarbons quench all the scintillation light in both xenon and argon. One can see that in this geometry the light output in xenon was observed to be at least a factor of 5 higher than in argon. In argon N_2 works as a wavelength shifter and the UV light lost is transformed into visible light so the net loss is minimal. This is not true for xenon, the reason may be buried in the fact that the ionizing potential of xenon is less than that of N_2, making it an energetically less favorable process. The results of this study were not very promising since it turns out that the gas admixtures (CO_2, CH_4) that improve the drift and diffusion also drastically cut down the scintillation yield.

Another serious problem is using scintillation light as time zero trigger is the phenomenon known as secondary scintillation. In addition to the primary scintillation there is always secondary scintillation in pure xenon, when the drifted electrons reach the anode wires. The

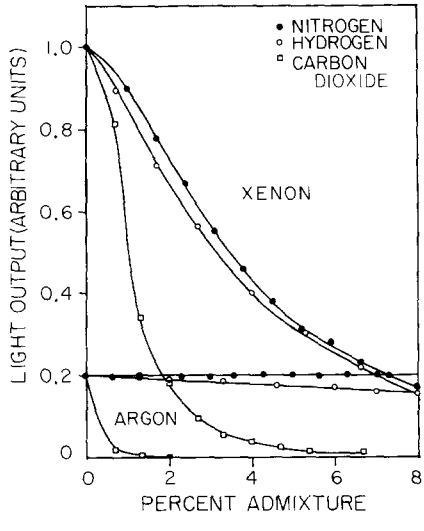

Fig. 3. The scintillation light yields of xenon and argon as a function of different gas mixtures.

accelerated electrons produce this scintillation light by collisions in the very strong electric field around the anode wires. Secondary scintillation starts well before the charge multiplication and the light intensity is typically a few orders of magnitude stronger compared to the primary scintillation at the working voltage. The background produced by the secondary scintillation makes the time zero triggering particularly difficult even with a very clever timing scheme. The far UV nature of the scintillation results in increased background problems by photoelectron emission from the wall of the detector. This was very clearly demonstrated by the signals from a 2.5 cm diameter cylindrical proportional counter. Fig. 4a shows the pulses with pure xenon. One can see the successive pulses which are generated by the photoelectrons produced from the detector when the UV photons from the secondary scintillation strike the wall. The separation of the pulses represent the drift time of the electrons from the wall to the anode wire. Fig. 4b shows the same pulses when the scintillation was quenched by mixing 1% CH_4, one can see that the secondary pulses associated with the scintillation have completely disappeared.

Using the same proportional counter we have studied different gas mixtures as a proportional counter gas. With pure xenon in the counter we achieved about 10% energy resolution for an ^{55}Fe X-ray (5.9 keV) source. However, the range of the working voltage was very small (50 V out of 1400 V for this geometry), and even within this working range the operation was not very stable against high voltage breakdown. With 5% admixture of CH_4, at the cost of scintillation light, xenon can be used as a very efficient proportional counter gas. This solves the problem of diffusion and increases the drift velocity as well. Since the scintillation is completely quenched by the admixture of CH_4, the associated problem of photoelectron emission is also eliminated. The price we pay for not having a time zero scintillation trigger is that we can not assign the absolute position of the track in the drift direction. However, it is obvious from the above discussion that maximizing the scintillation light is in direct contradiction to good imaging and energy resolution which are the main goals for a TPC.

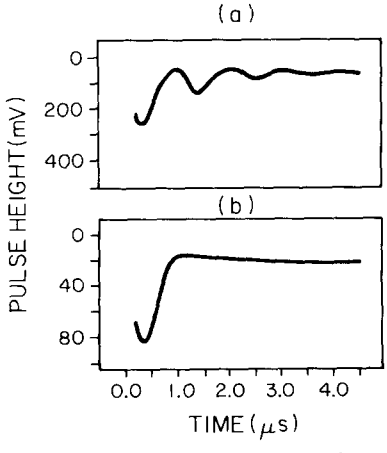

Fig. 4. (a) Signal from proportional counter with pure xenon. (b) Same signal with 1% admixture of CH_4.

3.2. Track reconstruction

The prototype TPC has been used for imaging tracks of various changed particles. We developed the electronics using standard drift chamber gas (90% Ar + 10% CH_4) at 1 atm. The time zero trigger in the cosmic ray muon tracks comes from two plastic scintillators sandwiching the TPC. Once we were reasonably satisfied with the electronics we replaced the fill gas with a Xe–CH_4 mixture. We started with 1% admixture of CH_4 and later increased it to 5% for stable performance against high voltage breakdown. This gas mixture worked very well and we could image tracks of charged particles (cosmic ray muon, alpha particles or electrons). Except for the cosmic ray muons no trigger was available and we started the image recording process by the first available signals from the anode wires. For diagnostic purposes, we also triggered by a randomly

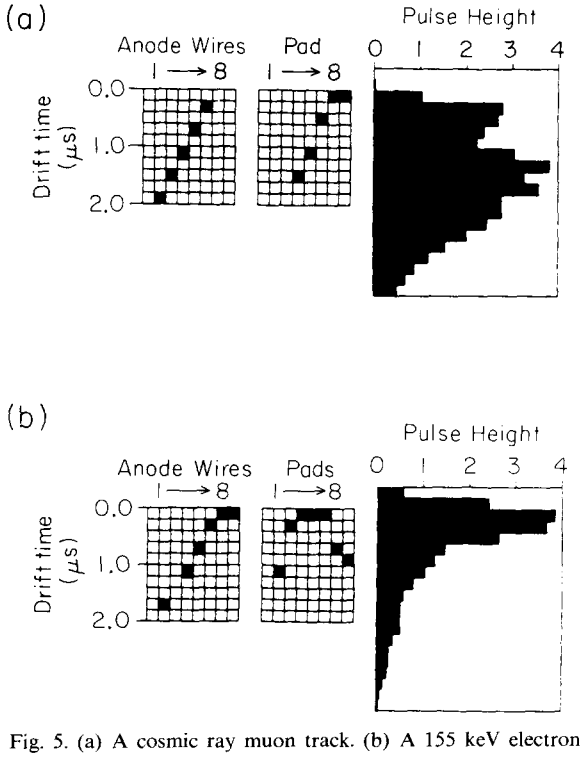

Fig. 5. (a) A cosmic ray muon track. (b) A 155 keV electron track.

chosen channel and reconstructed the part of the track which arrives to the readout system after the triggering. In figs. 5a and b a muon track and an electron track are shown. The 155 keV conversion electron from a ^{139}Ce source leaves a 10 cm long track in 1 atm of xenon, which is normally very erratic due to multiple scattering. We picked out a relatively straight track in order to demonstrate the resolution of the system. We expect the track resolution to improve significantly when we have digitizers on each channel. The first two columns in the figures show the projection of the tracks in xz and yz planes as a function of time, where x, y and z represent the anode wire, pad and the drift directions respectively. The drift distance z is given by the product of the drift velocity with the drift time shown in the figures.

3.3. dE/dx and the energy measurement

As mentioned earlier, there is no provision for energy measurements in this system. In the final design, track reconstruction, energy and dE/dx measurements will be carried out simultaneously. However, to get an idea of the energy and dE/dx we decided to look at the signal induced on the Frisch grid since the grid will pick up signals from all the anode wires, in the right order with time. The grid signal gives us information about the total energy and in some cases dE/dx. To do this we connected the grid to a preamplifier which kept it at virtual ground so that the drift field remained the same inside the TPC. The signal from the grid was digitized using a transient recorder (LeCroy TR 8837F) during an event, and examples are shown in the third column of figs. 5a and b. They show the time development of the charge collection in the anode wires. In a straight track, such as the muon track, this time development directly corresponds to dE/dx. In a zigzag track of electrons with multiple scattering, this is no longer true, since charges from different parts of the track may be collected at the same instance inducing a large unresolved pulse, if they lie on the sam drift plane. However, the integrated area in all the cases will corresponds to the total energy. An energy spectrum based on 10000 events for 155 keV electrons from a ^{139}Ce source is shown in fig. 6. The peak is resolved but the energy resolution is poor. This is not surprising since the grid has a very large capacitance and is consequently very noisy. Also the drift electric field is not very uniform around the edges since we used only two guard rings. Moreover, all the events were not fully contained in the drift volume because of the small size of the TPC. We expect to achieve about 10% energy resolution which is close to the theoretical limit in the proportional region. (Much better energy resolution is possible in ionization chambers were the energy resolution is limited by the Fano factor only.) The present

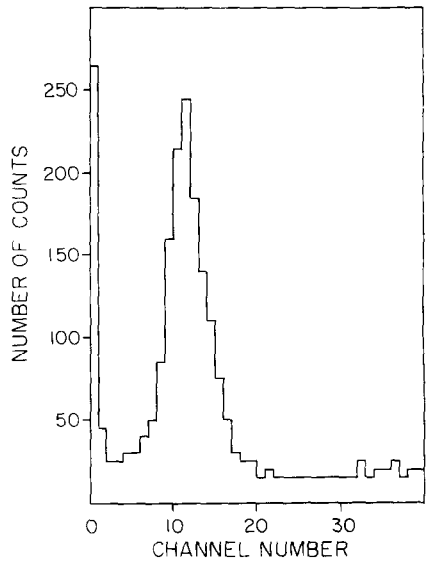

Fig. 6. Energy spectrum of 155 keV electron.

system is too small and the spatial resolution is too coarse to see the charge blob at the end of an electron track which is produced by the increased dE/dx for low energy electrons. However, on comparing the charge deposition per unit length in the minimum ionizing region (2.5 MeV) to a low energy electron (155 keV), we observed that the average charge deposition per unit length for the low energy electrons is roughly a factor of 4 higher.

4. Conclusion

The prototype xenon TPC has provided us with the necessary information required for the design of the next generation TPC. We have shown that imaging with good energy resolution is difficult to achieve while observing the scintillation light. Xenon with 5% or more admixture of CH_4 can be used as a fill gas for the TPC with good drifting properties and stability against high voltage breakdown. Tracks of various charged particles like alpha particles, cosmic ray muons and electrons were reconstructed using the available electronics. Although the system was not designed for energy or dE/dx measurement we could get qualitative information using the grid to collect the induced signals. We also designed a purification system suitable for the next generation TPC.

We are currently designing a 200 l xenon TPC, suitable to operate at 5 atm pressure. A typical track, simulated by Monte Carlo calculation [25], of a 1.25 MeV electron at 5 atm of xenon is shown in fig. 7. At least 400 channels will be required to resolve the charge blobs at both ends of a track which serves as a char-

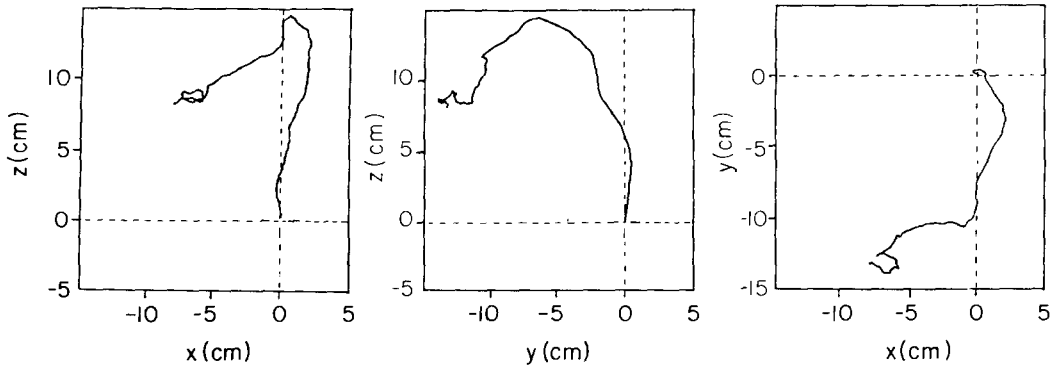

Fig. 7. The trajectory of a 1.25 MeV electron in 5 atm of xenon, ejected along the z axis from the origin, as simulated by Monte Carlo calculation. (a), (b) and (c) show the projections on the xz, yz and xy planes respectively.

acteristic signature of a true event. In this TPC about 30% of the total events will be fully contained in the active volume at 5 atm. The total number of ^{136}Xe atoms in the active volume will be 3×10^{23} which is comparable to the present generation of germanium experiments.

References

[1] M. Deutsch and O. Kofoed-Hansen, Experimental Nuclear Physics, vol. 3, ed., E. Segré (Wiley, New York, 1959) p. 427.
[2] S.P. Rosen and H. Primakoff, in Alpha-, Beta- and Gamma-spectroscopy, vol. 2, ed., K. Siegbahn (North-Holland, Amsterdam, 1965) p. 1499.
[3] D. Brymann and C. Picciotto, Rev. Mod. Phys. 50 (1978) 11.
[4] Yu.G. Zdesenko, Fiz. Elem. Chastits At. Yadra 11 (1980) 1364 [Sov. J. Part. Nucl. 11 (1980) 542].
[5] H. Primakoff and S.P. Rosen, Ann. Rev. Nucl. Sci. 31 (1981) 145.
[6] T. Kirsten and H.W. Muller, Earth Planet. Sci. Lett. 6 (1969) 271.
[7] M.G. Inghram and J.H. Reynolds, Phys. Rev. 78 (1950) 822.
[8] T. Kirsten, O. Schaeffer, E. Norton and R. Stoenner, Phys. Rev. Lett. 20 (1968) 1300.
[9] E.W. Hennecke, O. Manuel and D. Shabu, Phys. Rev. C11 (1975) 1378.
[10] E.W. Hennecke, Phys. Rev. C17 (1978) 1168.
[11] M.K. Moe, University of California at Irvine, Neutrino Report no. 133 (1984) to be published.
[12] F.T. Avignone, R.L. Brodzinski, D.P. Brown, J.C. Evans, W.K. Hensley, H.S. Miley, J.H. Reeves and N.A. Wogman, Phys. Rev. Lett. 54 (1985) 2309.
[13] A. Forster, H. Kwon, J.K. Markey, F. Boehm and H.E. Henrikson, Phys. Lett. 138B (1984) 301.
[14] E. Bellotti, O. Cremonesi, E. Fiorini, C. Liguori, A. Pullia, P. Sverzellati and L. Zanotti, Phys. Lett. 146B (1984) 450.
[15] F.T. Avignone, R.L. Brodzinski, D.P. Brown, J.C. Evans, W.K. Hensley, J.H. Reeves and N.A. Wogman, Phys. Rev. Lett. 50 (1983) 721.
[16] D.O. Caldwell, R.M. Eisberg, D.M. Grumm, D.L. Hale, M.S. Witherell, F. S. Goulding, D.A. Landis, N.W. Madden, D.F. Malone, R.H. Pehl. and A.R. Smith, Phys. Rev. Lett. 54 (1985) 281.
[17] H. Ejiri, N. Takahashi, T. Shibata, Y. Nagai, K. Okada, N. Kamikubota and T. Watanabe, Proc. Int. Symp. on Nuclear Spectroscopy and Nuclear Interactions, Osaka, Japan (1984) to be published.
[18] J.J. Simpson, P. Jagam, J.L. Campbell, H.L. Malm and B.C. Robertson, Phys. Rev. Lett. 53 (1984) 141.
[19] M. Mutterer, P. Grimm, H. Heckwolf, J. Pannicke, W. Speng and J.P. Theobald, Detectors in Heavy Ion Reaction, Lecture Notes in Physics 178, Proc., Berlin (1982).
[20] A.J.P.L. Policarpo, Phys. Scripta 23 (1981) 539.
[21] M. Salete S.C.P. Leite, Portugal Phys. 11 (1980) 53.
[22] M. Suzuki, J. Ruan (Gen) and S. Kubota, Nucl. Instr. and Meth. 192 (1982) 565.
[23] L.G. Christophorou, D.V. Maxey, D.L. McCorkle and J.C. Carter, Nucl. Instr. and Meth. 171 (1980) 491.
[24] A. Peisert and F. Sauli, CERN 84-08.
[25] T.L. Kwok, Senior Thesis, California Institute of Technology (1984).